Structural/Seismic Analysis of New and Spent Fuel Storage Racks

Technical Report

Non-Proprietary Version

September 2013

Copyright ⓒ 2013

Korea Electric Power Corporation &
Korea Hydro & Nuclear Power Co., Ltd
All Rights Reserved

Revision History

Revision	Page (Section)	Description
0	All	Original Issue

This document was prepared for the design certification application to the U.S. Nuclear Regulatory Commission and contains technological information that constitutes intellectual property.

Copying, using, or distributing the information in this document in whole or in part is permitted only by the U.S. Nuclear Regulatory Commission and its contractors for the purpose of reviewing design certification application materials. Other uses are strictly prohibited without the written permission of Korea Electric Power Corporation and Korea Hydro & Nuclear Power Co., Ltd.

ABSTRACT

This report provides the methodology and results of seismic and structural analysis of new and spent fuel storage racks which are intended to be used for NRC Design Certification of the APR1400.

TABLE OF CONTENTS

LIST OF TABLES

LIST OF FIGURES

Acronyms and Abbreviations

The abbreviations listed below have the following meanings where used;

ASME	American Society of Mechanical Engineers
NFSR	New Fuel Storage Rack
OBE	Operation Basis Earthquake
PSD	Power Spectrum Density
RG	Regulatory Guide
SFP	Spent Fuel Pool
SFSR	Spent Fuel Storage Rack
SRP	Standard Review Plan
SSE	Safe Shutdown Earthquake
USNRC	United States Nuclear Regulatory Commission
ZPA	Zero Period Acceleration

1.0 Purpose

The purpose of this report is to evaluate the structural integrity of the new and spent fuel storage racks under all postulated loading conditions for the APR1400. All evaluations follow the USNRC Standard Review Plan (SRP) [Ref. A.1], and the design specification [Ref. B.1 & B.2], whichever is more limiting. Result of stress evaluation according to ASME Section III, Subsection NF [Ref. A.2] shows that new and spent fuel storage racks of the APR1400 maintain the structural integrity.

2.0 Rack Layout and Description

2.1 New Fuel Storage Rack Description

Figure 2-1 shows the storage layout for the new fuel pool of the APR1400. The total storage capacity is 112 cells.

New fuel storage rack consists of two 7 cell x 8 cell modules. The new fuel storage rack is not submerged in water and support pedestal is fixed by stud bolts on the pool liner.

Figure 2-2 shows arrangement and direction of the new fuel storage rack. Material and principal dimension data of each rack used in analysis are summarized in section 6.1 of this report.

Figure 2-1 New Fuel Storage Rack Layout

TS

Figure 2-2 New Fuel Pool Layout Plan Dimensions

2.2 Spent Fuel Storage Rack Description

Figure 2-3 shows the storage layout for the spent fuel pool of the APR1400. The total storage capacity is 1792 cells. Spent fuel pool is separated into two areas of Region I and Region II.

Region I consists of four 8 cell x 8 cell rack modules and two 6 cell x 8 cell modules. Region II consists of nineteen 8 cell x 8 cell rack modules and 8 cell x 7 cell rack modules. It shows the very tight rack-to-rack and rack-to-wall gaps. Spent fuel storage racks are composed of modules with the different number of cell and installed in water. The spent fuel storage racks described above are free standing with pedestals resting on bearing pads.

Figure 2-4 show arrangement and direction of the spent fuel storage rack. Material and principal dimension data of each rack used in analysis are summarized in section 6.1 of this report.

Figure 2-3 Spent Fuel Storage Rack Layout

TS

Figure 2-4 Spent Fuel Pool Layout Plan Dimensions

3.0 Analytical Method

3.1 Time History Generation

The response of a free-standing rack module to seismic inputs is highly non-linear and involves a complex combination of motions (sliding, rocking, twisting, and turning), resulting in impacts and friction effects. Non-linear model requires 3-Dimensional transient dynamic analysis. Therefore, seismic load of response spectra specified in design specification should be converted to acceleration-time histories for three orthogonal directions which comply with the guidelines of the United States Nuclear Regulatory Commission (USNRC) Standard Review Plan (SRP) [Ref. A.1].

It converts Operating Basis Earthquake (OBE) and Safe Shutdown Earthquake (SSE) response spectrum specified in Ref. B.2 to acceleration – time history data satisfying requirements of NUREG-0800, SRP 3.7.1 [Ref. A.1]. This is specified in Appendix A of this report.

Acceleration – time history load for new and spent fuel storage racks seismic analysis of the APR1400 was adopted by converting the response spectrum load at Auxiliary Building Elevation 137'-6" and 114'-0", respectively.

3.2 Seismic Analysis

3.2.1 Analysis Overview

Spent fuel storage rack is located but not fixed at the bottom of spent fuel pool. There is a little gap between spent fuel assembly and walls of cell, which allows it to move horizontally. Although new fuel storage rack is fixed to the bottom of new fuel pool, a little gap between fuel assembly and walls of cell allows it to move horizontally. These structural features make fuel storage rack respond to external load with collusions, slip due to friction effects, tilting, and etc.

Since spent fuel storage rack is a structure submerged in water, adjacent rack is influenced by each other due to interaction by fluid flow between each storage rack, fuel assembly, and storage rack.

Linear methods, such as response spectrum analysis, cannot accurately simulate the structure such as non-linear response. Therefore, an accurate simulation is obtained by direct integration of the nonlinear response function and applying acceleration – time history of each direction at the same time.

Spent fuel storage rack of the APR1400 was used multi-rack analysis method. This method analyzes simultaneously the whole pool storage rack. New fuel storage rack did not use multi-rack analysis method because of same size and installed in air. However, its analysis process is similar to that of spent fuel storage rack.

Dynamic analysis of fuel storage rack was performed using finite element analysis program ANSYS (Ref.

E.1). Stress of each part was calculated by applying analysis result of ANSYS to material mechanics formula.

3.2.2 Analysis Considerations

Spent fuel storage rack has a non-linear characteristic kinematically. In actual analysis, using non-linear dynamic analysis model is adopted to obtain kinematic response and stress. This model reflects structural characteristic of each storage rack. Characteristic of non-linear dynamic analysis model of each storage rack should equate to motion characteristic of actual storage rack.

Analytical model of spent fuel storage rack shall be able to transfer momentum generated by motion of storage fuel assembly and simulate tilt of storage rack and impact of the tilt.
Also, it shall properly consider the fluid coupling effects by fluid in cell and fuel assembly, and gap between storage racks. Slip of pedestal is described as coulomb friction coefficient. Friction coefficient values vary according to condition of the friction surface. Generally, large friction coefficient generates large load and stress, while small friction coefficient augments sliding distance in the event of slip due to external load.
Many potential variables influence the rack analysis result. Therefore, the analysis must consider changes in potential variables so as not to undermine conservative.
The 3-Dimensional dynamic analysis model of storage rack includes variables such as following.

(1) Friction coefficient

Coefficient of friction has upper and lower limits, which are 0.8 and 0.2 respectively based on experimental data. Linear elements (friction) for each section are assigned for pedestal-to-pool bottom contact.

(2) Beam Element of Storage Rack

Storage rack is composed of linear elastic beam elements with stiffness against bending, rotation and tension.

(3) Impact phenomena

Compression-only spring elements, with gap capability, are used to provide for opening and closing of interfaces such as the pedestal-to-spent fuel pool interface, the fuel assembly-to-cell wall interface. The gap element is displayed as non-linear spring element. Restoring force is not proportional to displacement.

(4) Storing condition of Fuel assembly

The fuel assemblies are assumed to have same movement simultaneously so that impact load against the square pillar wall has conservative.

(5) Hydrodynamic effect

For hydrodynamic effect of the adjacent storage from storage in spent fuel pool, a common used formula [Ref. D.1] is adopted. This formula is based on the potential flow theory of Fritz [Ref. D.2] and calculates value of the hydrodynamic mass of two objects in the fluid.

New fuel storage rack has no hydrodynamic effect because it is installed in the air.

The kinematics phenomenon of storage rack in the spent fuel pool is indicated by analysis which includes hydrodynamic effect.

3.2.3 Multi-Rack Analysis Method

Analysis of fuel storage rack is performed in the process of analysis and development of model as follows;

a. Each storage racks is created in a 3-dimensional dynamic analysis model for time history analysis. This model includes hydrodynamic effects and non-linear element of inter-rack. It is combined with spent fuel pool and creates one 3-dimensional analysis model for analysis, the so-called “Multi-Rack Analysis Method”.
b. Various multi-rack analysis models were created from various physical conditions of friction coefficient, fuel storage conditions, and etc. Maximum displacement and load of each storage rack is obtained by a 3-dimensional time history analysis using multi-rack analysis model.
c. Stress is calculated using the general equation of material mechanics by obtained load from dynamic analysis. Calculated stress is evaluated based on the criteria in ASME Section III, Subsection NF [Ref. A.2].

3.2.4 Dynamic Analysis Model of Storage Rack

All non-linear characteristics and variables were considered when creating a dynamic analysis model of fuel storage racks. Details for dynamic analysis model of spent fuel storage rack are as follows.

a. Storage rack consists of bottom plate, body and pedestal. Each component was created as 3-dimensional elastic beam. Beam element indicates the dynamic characteristics of storage racks according to stiffness of storage rack. Details for dynamic characteristics of storage rack and elastic beam is shown in Appendix B of this report.
b. The fuel assemblies consist of 3-dimensional elastic beam and lumped mass. Lumped mass is assigned to upper, lower and center of storage rack. Each lumped mass has a degree of freedom in the horizontal direction. Vertical movement of fuel assembly is assumed to be the same as the vertical movement of the storage racks in the height from bottom plate. Center of gravity of fuel assembly is offset from center of storage rack according to state of fuel storage.
c. Hydrodynamic effect of inter-rack and rack-fuel assembly is represented by inertial force in terms of the kinetic energy of the system acting between them. Hydrodynamic mass of inter-rack and rack-fuel assembly was calculated by formula of Ref. D.2, and then was applied to analysis model.
d. In order to represent impact phenomenon of inter-rack and rack-fuel assembly, compression spring gap element between lumped mass was used. Gap element of horizontal direction was assigned to upper and lower of storage rack by two of inter-rack. The gap element of lower is located in the height of bottom plate. The initial distance between impacts object is determined by arrangement of storage rack, size of fuel assembly and cell. Stiffness is calculated in full analysis model.
e. Non-linear gap element is used in the representation of support pedestals in vertical direction. Linear friction spring element is used in the representation of support pedestals in horizontal direction. These elements are used in the representation of slant or sliding phenomenon of storage rack. Pool bottom was assumed completely rigid body, and to be in contact with support pedestals.
   Directional stiffness of support pedestals were assigned to spring element.

New fuel storage rack stores fuel assembly in the dry. Support pedestals are fixed by stud bolts. Dynamic analysis model of new fuel storage rack exclude hydrodynamic effects and non-linear effects of Support pedestals.

3.3 Detailed description of Element

3.3.1 Rack and Fuel Assembly Model

Figure 3-1 shows all nodes and elements for dynamic analysis model of spent fuel storage rack. Stiffness, length and mass of node of each rack differs each other according to size and characteristics. Node of each rack has displacement and rotation degree of freedom for each direction.

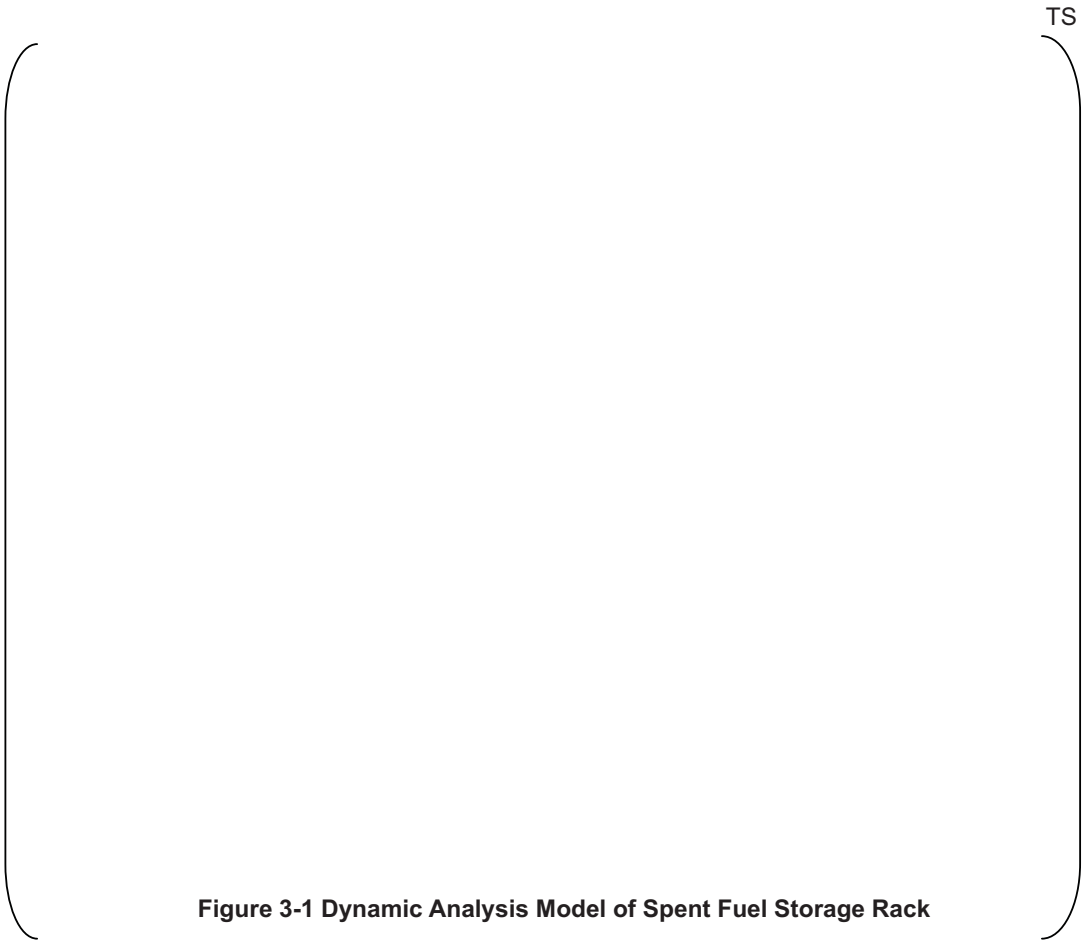

Figure 3-1 Dynamic Analysis Model of Spent Fuel Storage Rack

Fuel storage racks of the APR1400 are designed to accept 16 x 16 fuel assembly according to Appendix 4-2 of design specification [Ref. B.1]. Fuel assembly was modeled as elastic beam element and mass elements using three nodes. Two nodes are located in base plate and upper of storage rack each. One node is located in center of them. Three nodes are connected to gap element in the horizontal direction to consider impact phenomena according to relative motion of storage rack and fuel assembly.

If actual earthquake occurs, that spacer grid of fuel assembly would impact with cell walls of storage rack. It is expected to model with nodes of three fuel assembly has a spacer grid of three or more, a large impact load is generated than actual. Therefore, fuel assembly model of three nodes may have conservative.

Mass of each node in the fuel assemblies includes mass of all fuel assembly stored in each storage rack module. 1/4 of fuel assembly total mass was assigned to upper and lower nodes, respectively. And 1/2 of fuel assembly total mass was assigned to center node. All fuel assemblies were modeled together, which means all fuel assemblies are moved simultaneously in one direction. In actual case, each fuel assembly is expected to show an irregular movement. However, it became a conservative model for impact phenomenon by modeling all together.

As a result, fuel assembly is represented by three nodes and two elements. Each node has a displacement and rotation degree of freedom in each direction. Also it has a lumped mass element which represents weight of fuel assembly. Movement in vertical direction of fuel assembly is assumed to be same with vertical movement of bottom plate for storage rack.

Impact spring element of fuel assembly-to-rack interface is connected to upper, lower and center based on rack height. Linear friction spring element is connected to support pedestal-to-pool bottom interface.

Figure 3-2 shows mass element and impact spring of rack and fuel assembly, spring element of some support pedestal and impact spring element. Impact spring element was considered in case of impact of rack-to-pool wall.

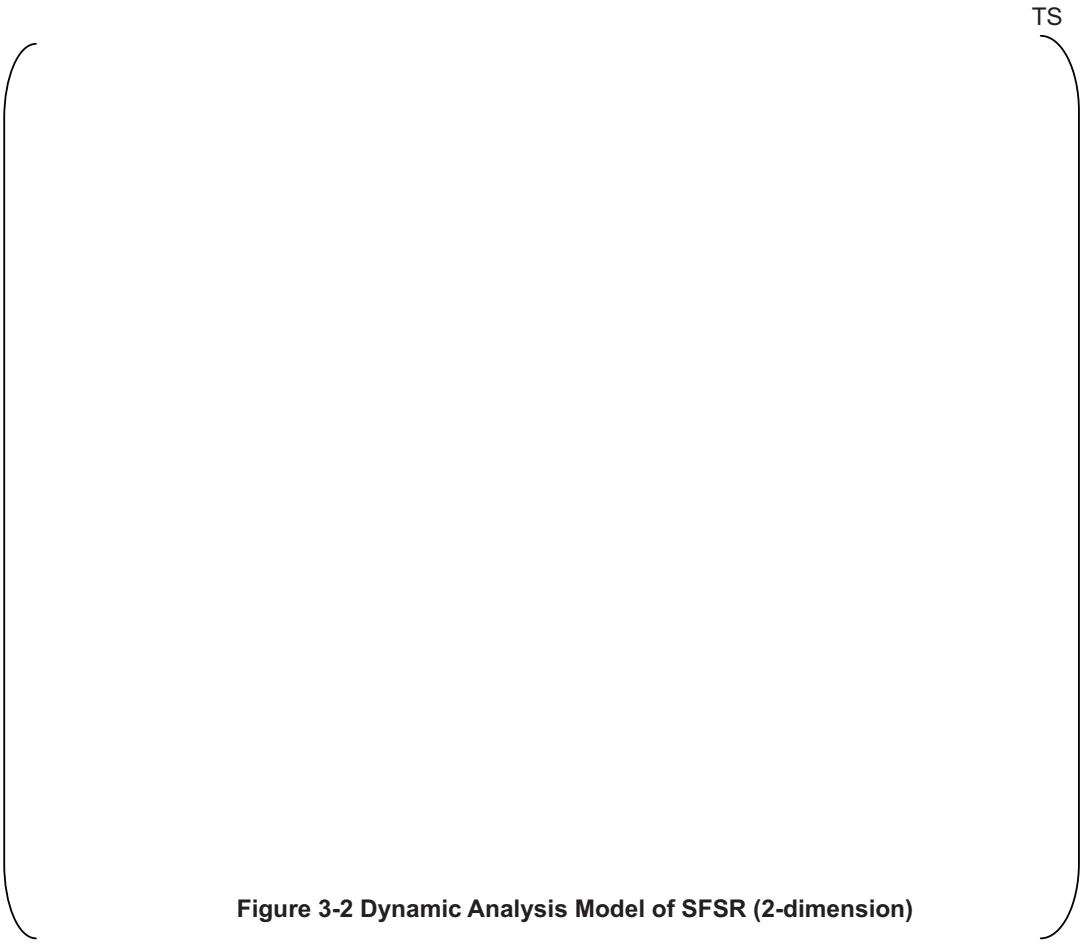

Figure 3-2 Dynamic Analysis Model of SFSR (2-dimension)

Dynamic analysis model of new fuel storage rack is shown in Figure 3-3. The new fuel storage rack is not submerged in water and support pedestal is fixed by stud bolts on the bottom. These characteristics are reflected at new fuel storage rack.

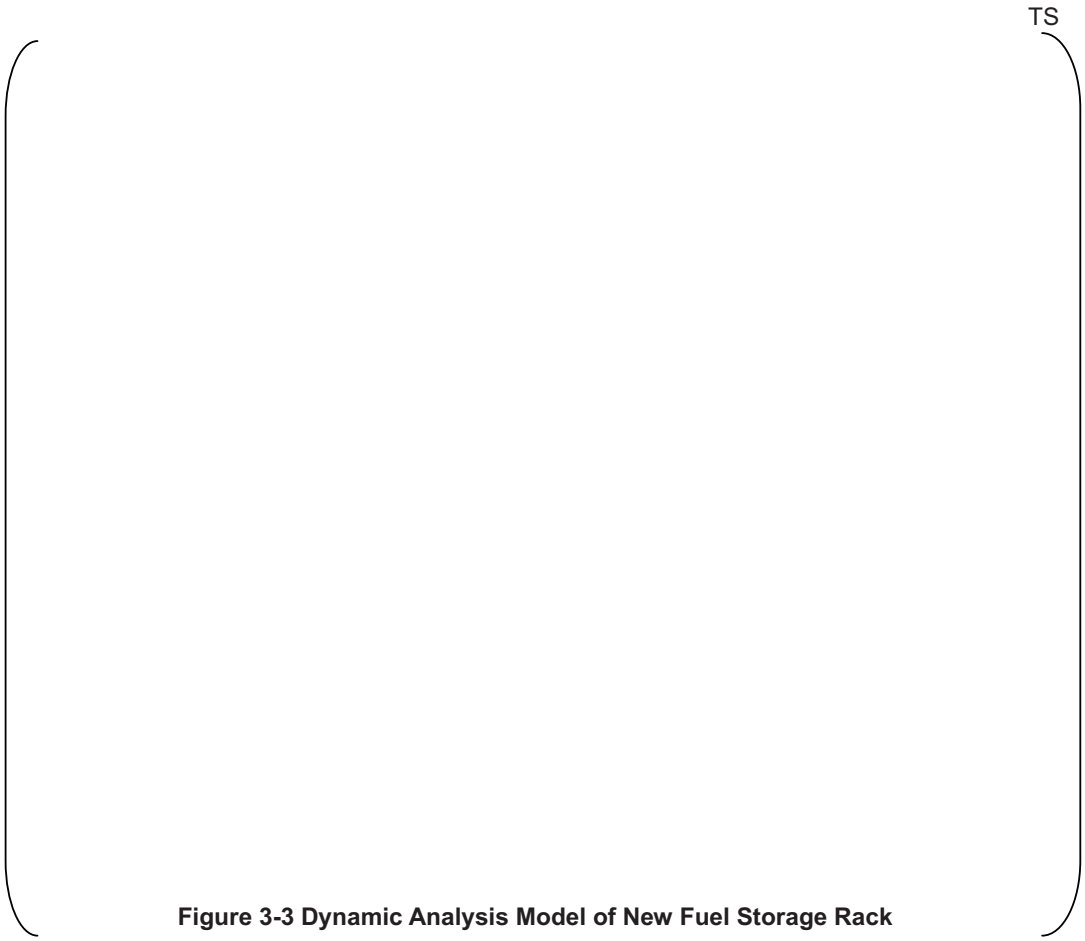

Figure 3-3 Dynamic Analysis Model of New Fuel Storage Rack

Figure 3-4 is multi-rack analysis model of spent fuel storage rack. It is overall dynamic analysis model of spent fuel storage rack created by combining each region for model shown in Figure 3-1.

TS

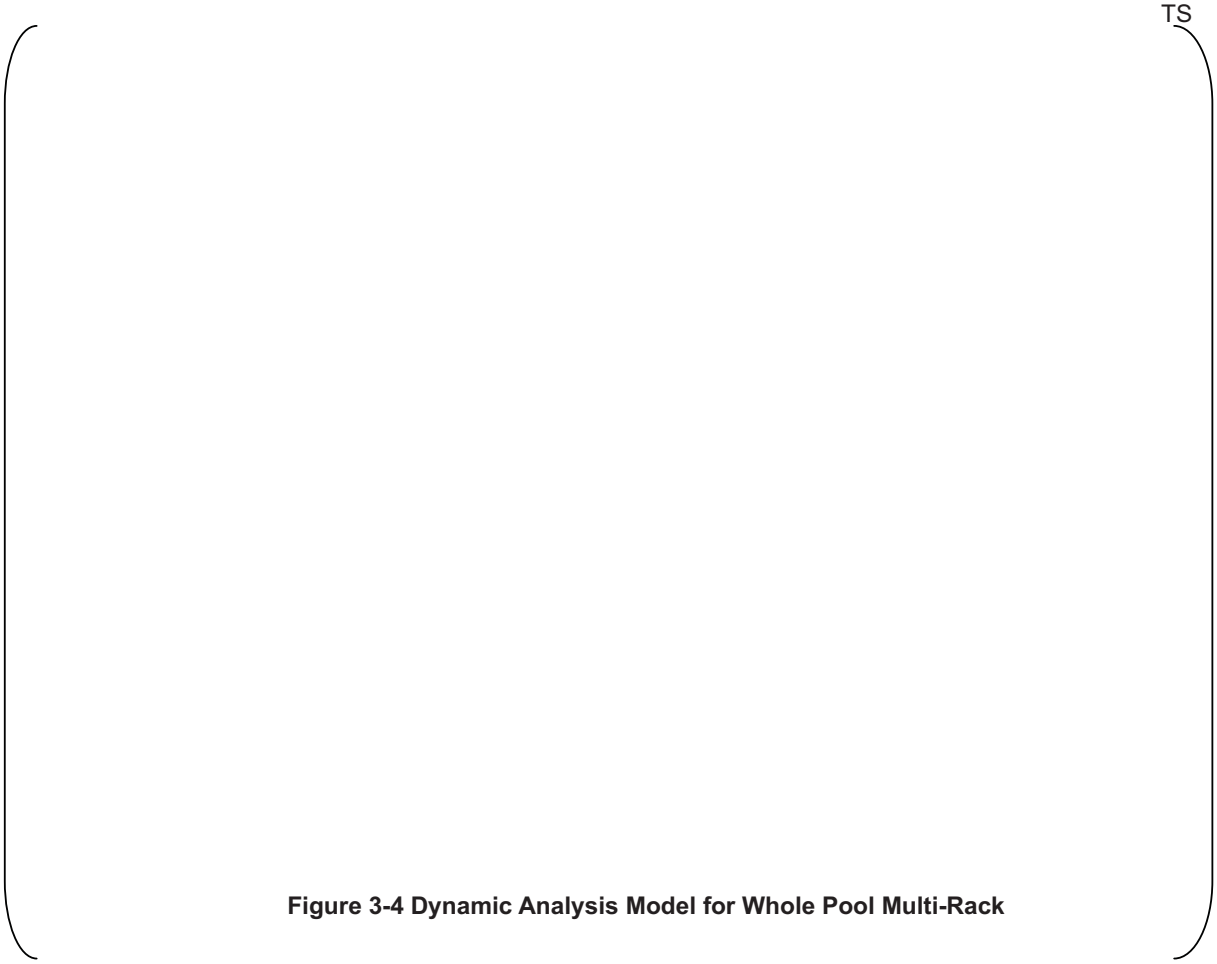

Figure 3-4 Dynamic Analysis Model for Whole Pool Multi-Rack

3.3.2 Hydrodynamic Mass

If external load like earthquake or local motion of internal occurs, spent fuel storage rack is influenced by fluid movement, because it is submerged in water. This phenomenon is called fluid coupling effect. The closer objects adjoin each other, the larger fluid coupling effect is as described in Ref. D.2. Each rack was assigned densely at spent fuel pool. Therefore, fluid coupling effect acts strongly on adjacent rack by cooling water of spent fuel pool.

Multi-Rack analysis describes simultaneously 3-dimensional movement of all rack modules. Therefore, it is possible to indicate phenomenon caused by fluid flow generated in the interaction between rack, rack and pool wall.

Hydrodynamic mass of fluid is considered because fluid exists between fuel assembly and cell of rack. Hydrodynamic mass acting between them due to fluid flow is calculated using formula of Ref. D.3.

Hydrodynamic mass of cell and fuel assembly, between each rack is calculated as following method.

(1) Between cell and fuel assembly

Fuel assembly consists of several fuel rods and guide tube, it is supported by spacer grid. Hydrodynamic effect was calculated assuming cylinder of long cylindrical whose centers match with each other. Hydrodynamic mass acting in two rigid body center match and liquid filled therein is represented using following formula of Ref. D.3.

$$\begin{pmatrix} F_1 \\ F_2 \end{pmatrix} = \begin{bmatrix} -M_H & M_1 + M_H \\ M_1 + M_H & -(M_1 + M_2 + M_H) \end{bmatrix} \begin{pmatrix} X_1'' \\ X_2'' \end{pmatrix}$$

$$M_H = \left[\frac{R_2^2 + R_1^2}{R_2^2 - R_1^2} \right] \pi \rho R_1^2 h$$

Where,

F_1, F_2 = Force of fluid acting respectively inside and outside the structure

M_1 = Mass of fluid was drained by internal structure

M_2 = If internal structure does not exist, mass of fluid present in external structure

X''_1, X''_2 = Absolute acceleration of each inside and outside of structure

M_H = Hydrodynamic mass

R_2 = Equivalent radius of storage box, convert cell width into radius

R_1 = Equivalent radius of fuel assembly, convert distance between fuel rods of outermost into radius

h = Length of fuel assembly

ρ = Density of fluid

Hydrodynamic mass is assigned to upper and lower node by 1/4 and center node by 1/2 respectively because cell and fuel assembly consist of three nodes. Calculated mass according to above formula means mass between one cell and fuel assembly. Therefore, it is applied to analysis model by multiplying the number of fuels being stored.

(2) Hydrodynamic mass effect of rack-to-rack and rack-to-pool wall.

Spent fuel pool has twenty-nine racks. Figure 2-1 shows dimension of rack-to-rack and rack-to-pool. Hydrodynamic mass between rack-to-rack and rack-to-pool wall is calculated based on height of rack, density of fluid and gap of adjacent racks assuming fluid is filled at between two objects consisting of rigid body, and center is eccentric.

If there is storage rack with one or more separate gap at surface in contact with adjacent rack, hydrodynamic mass was calculated based on average gap with weight. Hydrodynamic mass has weighted value according to overlapping length of rack surface.

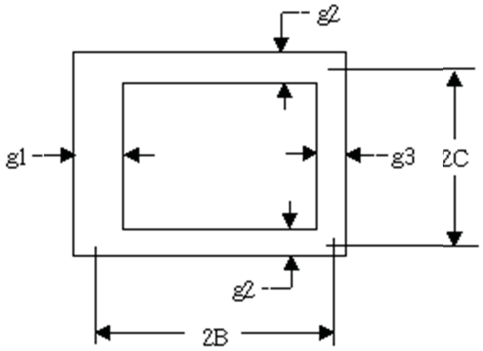

$$M_{H(horiz)} = 2\rho h C^2 \left[\frac{C}{3g_1} + \frac{C}{3g_3} + \frac{2B}{g_2} \right]$$

$$M_1 = \rho h (2C - g_2) \left[2b - (\frac{g_1 + g_3}{2}) \right]$$

$$M_2 = \rho h (2C + g_2) \left[2b + (\frac{g_1 + g_3}{2}) \right]$$

Where, h means height of storage rack, ρmeans density of fluid, g1, g2, g3 means gap.

If gap (g2) is different from each other, hydrodynamic mass is calculated using average gap. If two or more racks overlap each other, hydrodynamic mass is calculated using average gap with weighted value.

3.3.3 Detailed description of Stiffness Element

Stiffness elements of two types are used to rack model. First, 3-dimensional elastic beam element was used to represent behavior of each rack. Secondly, linear friction spring element was used to consider gap. This spring element was used to calculate load in horizontal direction by friction force between pedestal legs of storage rack and bottom of pool, collision load of rack wall and fuel assembly, impact load of between rack, rack and pool wall.

Impact phenomenon can be represented as a contact element of ANSYS (Ref. E.1). This element is capable of supporting only compression in the direction normal to the surfaces and shear (Coulomb friction) in the tangential direction. The element has three degrees of freedom at each node for displacement of three directions(x, y & z). A specified stiffness acts in the normal and tangential directions when the gap is closed and not sliding.

Figure 3-2 shows 2-dimensional analysis models for understanding of 3-dimensional analysis model.

(1) Impact of fuel assembly and rack

Fuel assembly is located in base plate of rack without any support structure and close interval. If earthquake occurs, fuel assembly can possible to impact with each cell of rack. This collision is effected by impact load. It influences dynamic behavior of rack. Contact element was connected to each node of fuel assembly beam model.

The gap between fuel assembly and storage rack considered in contact element was based on space size between cell and grid of fuel assembly. In order to consider impact load of fuel assembly and rack, the overall stiffness can be applied assuming series spring connection of stiffness of fuel assembly's spacer grid and local stiffness of cell in horizontal direction. However, only stiffness of fuel assembly is applied in this report in consideration of conservative. Spring element in Figure 3-2 has a local stiffness (Ki) to indicate collision phenomenon of rack wall and fuel assembly.

Fuel assembly is composed of eleven spacer grids. It is applied to seismic analysis model by multiplying the number of fuel assemblies stored in total grid stiffness.

(2) Vertical collision of rack and bottom of pool

Contact element was connected to four nodes corresponding to support of rack. Stiffness of vertical impact load can be applied assuming series spring connection of vertical stiffness of rack, embedment/liner plate of pool and pool concrete. In this case, structure analysis shall be performed on each part (support, embedment/liner plate, storage pull concrete) to obtain stiffness of each.

Only stiffness (Ks) of support for rack as stiffness for collision between fuel assembly and rack was applied in this report for conservative.

Support pedestal and bottom of pool generate horizontal direction load by friction. Compression load (N) generated between pedestal and bottom of pool and maximum friction load (μN) by friction coefficient (μ) is reflected with horizontal direction stiffness (Kf). In transient analysis, Compression load (N) is calculated at analysis step of each time.

(3) Collision of rack-to-rack and rack-to-pool wall

Collision of rack is equally applied to rack-to-rack and rack-to-pool wall assuming series spring connection of horizontal stiffness of rack.

3.3.4 Friction coefficient

Because spent fuel storage rack is placed but not fixed on pool, slip could occur between rack and bottom of pool. Coefficient of friction (COF) values are assigned at each interface, which reflect the realities of wetted stainless steel-to-stainless steel contact. The mean value of coefficient of friction is 0.5, and the limiting values are based on experimental data, which has been found to be bounded by the values 0.2 and 0.8 [Ref. D.3]. Low friction coefficient can increase distance of slip and high friction coefficient can increase load of rack.

4.0 Assumption and Load Combination

4.1 Assumptions

The following assumptions are used in the analysis:

a. Fluid damping and drag are neglected in consideration of conservative.

b. Sloshing effect of spent fuel pool surface is neglected, because rack is a submerged structure deep in the fluid.

c. Fuel assembly was considered as 3-dimensional elastic beam, concentrated mass located in upper, lower and middle of rack. Each concentrated mass has a degree of freedom in horizontal direction. Vertical movement of fuel assembly was assumed to be equal to vertical movement of rack in height of bottom plate.

d. When earthquake occurs rack is affected by irregular movement of fuel assembly. All fuel assemblies were assumed to move as one object within rack for conservative evaluation.

4.2 Lad and Load Combinations

The applicable load and load combination of structural analysis for rack are defined as follows in accordance with design specification [Ref. B.1] and USNRC NUREG-0800, SRP 3.8.4, Appendix D [Ref. A.1]. The acceptance criteria are defined in ASME Code Section III, Subsection NF [Ref. A.2].

Table 4.1 Load Combinations for Rack Analysis

Load Combination	Service Limit
D + L D + L + T_o D + L + T_o + E	Level A
D + L + T_a + E D + L + T_o + P_f	Level B
D + L + T_a + E' D + L + F_d	Level D The functional capability of the fuel racks should be demonstrated.

Where,

D : Dead weight including fuel assembly weight
L : Live load (not applicable for the fuel rack, since there are no moving objects in the rack load path). Note that it is accepted practice to consider the fuel weight as a dead weight.
E : Operating Basis Earthquake (OBE)
E' : Safe Shutdown Earthquake (SSE)
T_o= Differential temperature induced loads, based on the most critical transient or steady state condition under normal operation or shutdown conditions.
T_a= Differential temperature induced loads, based on the postulated abnormal design conditions
F_d= Force caused by the accidental drop of the heaviest load from maximum possible height.
P_f= Force on the racks caused by postulated stuck fuel assembly. This force may be caused at any angle between horizontal and vertical.

Thermal load by Ta and To generates local stress in spent fuel storage rack. If one cell stores fuel assembly releasing maximum heat and adjacent cell does not store fuel assembly in rack, then rack receives the highest thermal stress. Thermal stress is caused by temperature difference of cooling water flowing in adjacent cell forming a common wall. Secondary stress (thermal stress) caused by this is limited to wall of adjacent cell.

5.0 Allowable Criteria

Structural analysis of fuel storage rack shall take into account all load acts in fuel storage rack in accordance with Regulatory Guide 1.13 [Ref. A.4] and USNRC NUREG-0800, Standard Review Plan [Ref. A.1]. This includes loads on fuel storage rack when fuel assembly is normally stored in fuel storage rack; when operating basis earthquake or safe shutdown earthquake occurs; when the fuel assembly or others handled on storage rack falls. The principal design criteria of storage rack are as follows.

5.1 Kinematic Criteria

Because spent fuel storage rack is installed autonomously, overturn or slip can happen due to external load. Design criteria for this are shown in Section 3.8.5 of Standard Review Plan [Ref. A.1]. For overturn and slip of fuel storage rack due to external load, minimum safety factor of 1.5 or 1.1 depending on each combination condition of load shall be secured. Safety factor is ratio of maximum rotational angle obtained from time history analysis and minimum angle in which storage rack can be overturned in each direction.

5.2 Stress Limit Criteria

ASME Section III, Appendix F and Subsection NF are applied as stress limit criteria of fuel storage rack as follows.

5.2.1 Normal Conditions (Level A)

(i) Stress in Tension [NF-3322.1(a)]

Allowable stress in tension on a net section is given by.

$$F_t = 0.6\ Sy$$

where,

S_y = Yield strength of material at a given temperature (F_t is equivalent to primary membrane stress)

(ii) Stress in Shear [NF-3322.1(b)]

Allowable stress of cross sectional area to resist shear force is as follows.

$$F_v = 0.4\ Sy$$

(iii) Stress in Compression [NF-3322.1(c)]

Allowable compressive stress of total cross sectional area of a member under compressive load in axial direction is as follows.

$F_a = Sy\ (0.47 - kl/444r)$

Where, $kl/r < 120$ for all sections

l = unsupported length of component.

k = length coefficient which gives influence of boundary conditions, e.g.

k = 1 (simple support both ends)

k = 2 (cantilever beam)

k = 0.5 (clamped at both ends)

r = radius of gyration of component

(iv) Stress in Bending [NF-3322.1(d)]

The allowable bending stress resulting from tension and compression of the farthest point from center to bending member of box type shall not be exceeding bending stress as follows.

$F_b = 0.66\ Sy$

(v) Combined stress (Combined Bending and Compression Loads) [NF-3322.1(e)]

Combined bending and compression on a net section satisfies

$$f_a/F_a + C_{mx}f_{bx}/D_xF_{bx} + C_{my}f_{by}/D_yF_{by} < 1.0$$

where, f_a = Direct compressive stress in the section

f_{bx} = Maximum bending stress along x-axis

f_{by} = Maximum bending stress along y-axis

$C_{mx} = 0.85$

$C_{my} = 0.85$

$D_x = 1 - (f_a/F'_{ex})$

$D_y = 1 - (f_a/F'_{ey})$

$F'_{ex,}\ F'_{ey} = (\pi^2 E)/(2.15\ (kl/r)_{x,y}^2)$

and subscripts x and y reflect the particular bending plane

(vi) Combined stress (Combined Flexure and Tension Loads) [NF-3322.1(e)]

Combined flexure and tension/compression on a net section satisfies

$$(f_a/0.6\ Sy) + (f_{bx}/F_{bx}) + (f_{by}/F_{by}) < 1.0$$

(vii) Welds [Table NF-3324.5(a)-1]

Allowable maximum shear stress on the net section of a weld is given by:

$$F_w = 0.3\ S_u$$

where, S_u is the material ultimate strength at temperature.

For the area in contact with the base metal, the shear stress on the gross section is limited to $0.4S_y$.

5.2.2 Upset Conditions (Level B)

Allowable stress can be increased by coefficient suggested in Table NF-3523 [Ref. A.2] of ASME Section III, Subsection NF for Level B stress limit. However, allowable stress of Level A is used in this report for conservative.

5.2.3 Faulted (Abnormal) Conditions (Level D)

Section F-1334 of ASME Section III, Appendix F [A.2], states that limits for the Level D condition are the smaller of 2 or $1.167S_u/S_y$ times the corresponding limits for the Level A condition if $S_u > 1.2S_y$, or 1.4 if S_u is less than or equal to $1.2S_y$ except for requirements specifically listed below. S_u and S_y are the ultimate strength and yield strength at the specified rack design temperature. Examination of material properties for 304L stainless demonstrates that 1.2 times the yield strength is less than the ultimate strength. Therefore, the 1.4 increase will not apply for 304L stainless, and since the value of $1.167S_u/S_y$ is equal to 3.63, the smaller multiplier (2.0) controls.

Exceptions to the above general multiplier are the following.

(i) Tensile stress shall be below the smaller value between 1.2Sy and 0.7Su.

(ii) Stresses in shear shall not exceed the lesser of $0.72S_y$ or $0.42S_u$. In the case of the material used here, $0.72S_y$ governs.

(iii) Combined Axial Compression and Bending - The equations for Level A conditions shall apply except that:

F_a = 2/3 x Buckling Load, and F'_{ex} and F'_{ey} may be increased by the factor 1.65.

(iv) For welds, the Level D allowable maximum weld stress is not specified in Appendix F of the ASME Code. An appropriate limit for weld throat stress is conservatively set here as:

$F_w = (0.3\ S_u)$ x factor

where,

factor = (Level D shear stress limit)/(Level A shear stress limit)

= $0.72 \times S_y / 0.4 \times S_y = 1.8$

5.3 Stress Coefficient

Stress coefficient calculates the ratio of allowable stress to the calculated stress for the combined and each load according to ASME Section III, Subsection NF. In case the calculated value is less than 1, it is considered to meet stress limit requirement for each operating condition. In this report, stress coefficient below was calculated using load combination.

FACT 1 = Stress coefficient of member receiving bending and axial direction compression at the same time

FACT2 = Stress coefficient of member receiving bending and axial direction tensile at the same time

FACT3 = Stress coefficient of net sectional area to resist shear force

6.0 Input Data

6.1 Input Data of Rack

Dimension and shape of rack used in this analysis are in accordance with the design drawing [Ref. F] and are summarized as follows.

TS

Table 6.1 Rack Module Data

TS

Table 6.2 Rack Details

Physical characteristics and weight of fuel assembly used for the APR1400 was applied based on Ref. B.1.

TS

Table 6.3 Fuel Assembly Data

6.2 Material Properties of Rack

Primary properties of rack are obtained as follows from Ref. A.3.

Table 6.4 Material Properties

Cells (@200 °F)			
Material	Young's Modulus E (psi)	Yield Strength Sy (psi)	Ultimate Strength Su (psi)
SA-240 Type 304L	27.5E+06	21,400	66,100
Support pedestal and base plate (@200 °F)			
SA-240 Type 304L (support pedestal and base plate)	27.5E+06	21,400	66,100
SA-564 Grade 630 (Bolt part)	27.8E+06	106,300	140,000

7.0 Analysis

Dynamic analysis was performed on the loading condition below according to fuel storage condition, friction coefficient and variety of seismic load considering variables of Section 3.0 in this report.

Table 7.1 List of Rack Simulations

Analysis Number	Variety of Storage Rack	Fuel storage condition	Variety of Earthquake	Friction Coefficient
1	New Fuel Storage Rack (NFSR)	Full Storage	OBE	N/A
2		Full Storage	SSE	N/A
3	Spent Fuel Storage Rack (SFSR)	Full Storage	OBE	0.2
4		Full Storage	OBE	0.5
5		Full Storage	OBE	0.8
6		Full Storage	SSE	0.2
7		Full Storage	SSE	0.5
8		Full Storage	SSE	0.8

8.0 Analysis Result

8.1 Time History Analysis Result

Time history analysis result was performed according to each load conditions. Analysis result is attained by load and displacements are summarized as follows.

8.1.1 Displacement of Rack

Table 8.1 Displacement of Storage Rack

1) Maximum absolute displacement (Horizontal direction)

Storage Rack	Displacement [mm (in.)]	Time (sec)	Direction	Storage Rack Number	Friction Coefficient	Storage Condition of Fuel	Type of Seismic
NFSR	10.8 (0.425)	3.405	N-S	N/A	N/A	Total Storage	SSE
SFSR	94.9 (3.735)	14.424	N-S	B6-2	0.2	Total Storage	SSE
	47.2 (1.858)	14.305	N-S	B10	0.5	Total Storage	SSE
	28.8 (1.134)	14.185	N-S	B5-6	0.8	Total Storage	SSE

2) Maximum relative displacement (Direction to be close to each other –Minus direction to analysis result)

Storage Rack		Displacement [mm (in.)]	Time (sec)	Direction	Storage Rack Number	Friction Coefficient	Storage Condition of Fuel	Type of Seismic
NFSR		N/A	N/A	N/A	N/A	N/A	N/A	N/A
SFSR	Region I	-42.8 (-1.684)	10.12	N-S	A1-2 to A2-2	0.2	Total Storage	SSE
		-20.4 (-0.804)	17.98	N-S	A1-2 to A2-2	0.5	Total Storage	SSE
		13.6 (-0.536)	10.09	N-S	A1-2 to A2-2	0.8	Total Storage	SSE
	Region II	-4.8 (-0.187)	17.13	E-W	B-9 to B-10	0.2	Total Storage	SSE
		-3.4 (-0.133)	5.105	E-W	B1-1 to B2-1	0.5	Total Storage	SSE
		-4.6 (-0.179)	4.261	E-W	C3 to C4	0.8	Total Storage	SSE

3) Maximum absolute displacement (Rotation)

3.735 Degree (B6-2 Module, Friction coefficient 0.2, Total storage)

Maximum displacement for upper of spent fuel storage rack is 94.9 mm (3.735 in.) and it is generated at N-S direction of B6-2 rack in 14.424 seconds as shown Table 8-1 of this report. Relative displacement of between adjacent racks of Region I is maximum 42.8 mm (1.684 in.) at direction to be close to each other (minus direction). It is generated at N-S direction of between A1-2 and A2-2 rack in 10.12 seconds.

Minimum Gap of outmost rack and pool wall is 716.6 mm (28.2 in.) in N-S direction and 835.4 mm (32.9 in.) in EW direction as shown in Figure 3-6. Therefore, impact with outmost rack and pool wall does not occur because maximum displacement 94.9 mm (3.735 in.) of rack lies within installation gap. Installation gap of between rack and rack cell is not fixed. But minimum gap for Region I is 60.0 mm (2.36 in.) in N-S direction and 60.0 mm (2.36 in.) in E-W direction, and 30.0 mm (1.18 in.) in N-S direction and 1.18 inch (30.0 mm) in E-W direction for Region II. Therefore, impact with between rack cells does not occur because maximum relative displacement 42.8 mm (1.684 in.) of Region I and 4.8 mm (0.187 in.) of Region II racks lies within installation gap.

Actually, Impact of rack-to-rack occurs at bottom plate because rack is installed in a way bottom plates are in contact with each other. Upper of rack impact is unlikely to happen. Impact between bottom plates is evaluated in section 8.1.3.1 of this report.

Rotation angle for upper of rack was used for evaluation on overturn of rack. Displacement toward rotation angle for upper of rack was calculated maximum 3.735^{o} as shown in Table 8.1 of this report. In order overturn of rack to happen, below rotation angle is required.

$$\tan^{-1}\left[\frac{h/2}{d/2}\right] = \tan^{-1}\left[\frac{4775/2}{1800/2}\right] = 69.3^{o}$$

Where, *h* means height of rack, *d* means width of rack. It has a safety factor for overturn of 69.3^{o} / 3.735^{o} = 18.5.
Therefore, it satisfies allowable criteria. Safety factor should be greater than 1.5. As a result, overturning of rack module does not occur.

8.1.2 Support Pedestal Load of Rack

Maximum horizontal and vertical load generated on support pedestal at the application of seismic load are summarized in Table 8.2 and 8.3 of this report, it was used to structural integrity evaluation of support pedestal and rack.

Table 8.2 Result Summary (Maximum Total Load per Module)

Storage Rack	Type		Horizontal direction (lbf)	Vertical direction (lbf)	Friction Coefficient	Storage Condition	Type of Seismic
NFSR	7 x 8		442,200	171,300	N/A	Total Storage	OBE
	7 x 8		513,100	223,900	N/A	Total Storage	SSE
SFSR	A1	8 x 8	121,000	153,000	0.8	Total Storage	OBE
	A2	6 x 8	95,900	120,000	0.8	Total Storage	OBE
	B1~10	8 x 8	116,000	145,000	0.8	Total Storage	OBE
	C1~4	8 x 7	106,000	132,000	0.8	Total Storage	OBE
	A1	8 x 8	382,000	597,000	0.8	Total Storage	SSE
	A2	6 x 8	324,000	510,000	0.8	Total Storage	SSE
	B1~10	8 x 8	471,000	592,000	0.8	Total Storage	SSE
	C1~4	8 x 7	380,000	532,000	0.8	Total Storage	SSE

(*) The loads on SSE condition include peak load due to impact which is secondary stress component.

Table 8.3 Result Summary (Maximum Total Load per Pedestal)

Storage Rack	Type		Horizontal direction (lbf)		Vertical direction (lbf)	Friction Coefficient	Storage Condition	Type of Seismic
			E-W	N-S				
NFSR	7 x 8		136,700	89,570	42,830	N/A	Total Storage	OBE
	7 x 8		170,000	148,400	55,980	N/A	Total Storage	SSE
SFSR	A1	8 x 8	30,200	29,300	38,200	0.8	Total Storage	OBE
	A2	6 x 8	22,700	23,000	30,100	0.8	Total Storage	OBE
	B1~10	8 x 8	28,900	28,700	36,100	0.8	Total Storage	OBE
	C1~4	8 x 7	26,100	25,500	33,100	0.8	Total Storage	OBE
	A1	8 x 8	100,000	51,500	149,000	0.8	Total Storage	SSE
	A2	6 x 8	68,500	73,500	128,000	0.8	Total Storage	SSE
	B1~10	8 x 8	119,000	60,500	148,000	0.8	Total Storage	SSE
	C1~4	8 x 7	95,300	39,400	133,000	0.8	Total Storage	SSE

8.1.3 Impact Load of Rack

A freestanding rack, by definition, is a structure subject to potential impacts during a seismic event. Also, impacts may arise from rattling of the fuel assemblies between rack cell and fuel assembly. Therefore, possibility of local impact was evaluated for rack-to-rack, between pool wall and pool and between rack cell and fuel assembly. Evaluation results are as follows.

8.1.3.1 Impact of Rack-to-Rack

Generally, the racks are installed together as closely as possible. Prominent bottom plate of fuel assembly for the APR1400 is installed almost in contact with adjacent bottom plate. According to analysis result, impact occurs not between wall of pool and upper of rack, but between bottom plates of racks. However, deformation of rack cell due to impact between racks does not occur.

Impact load by collision was calculated maximum 1,343.4 kN (0.302E+06 lbf) at bottom plate as shown in Table 8.4 of this report. Collision of bottom plate occurs at edge of bottom plate. The overall effect of storage is expected to be insignificant in consideration of resistance for compressive force of edge plate. Impact load is dispersed in a contact part of support pedestal and adjacent bottom plate by local deformation that occurs at the time of a collision. . Assuming that collision locally occurs over 5 inch width, when applying primary membrane stress criteria of level D to 6.5 inch thickness of support pedestal and bottom plate, it withstands a load of 1.2* (21,400) psi * (6.5) in. * (5) in. = 3,712.5 kN (0.8346E+06 lbf). Integrity of bottom plate is maintained because this load is greater than maximum impact load.

8.1.3.2 Impact of Rack-to-Pool Wall

According to analysis result of maximum displacement by seismic load, rack-to-pool wall does not occur.

Table 8.4 Maximum Impact Load Summary

Storage Rack	Component	Direction	Impact Load (lbf)	Storage Rack Number (Module)	Impact Load per Cell (1) (lbf)	Impact Load of Fuel support grid (2) (lbf)	Friction Coefficient	Storage Condition	Type of Seismic
NFSR	Fuel Assembly	EW	461,600	-	8,243	750	-	Total Storage	SSE
		NS	491,500	-	8,777	798	-	Total Storage	SSE
SFSR	Bottom Plate	Side	302,000	C1 (8x7)	-	-	0.2	Total Storage	SSE
	Fuel Assembly	EW	1,600,000	A1-1 (8x8)	25,000	2,273	0.8	Total Storage	SSE
		NS	1,190,000	A1-2 (8x8)	18,594	1,690	0.8	Total Storage	SSE

Notes:
(1) Impact load per cell = Side impact load/Number of stored fuel
(2) Impact load of fuel support grid = Impact load per cell/ Number of support grid

8.1.3.3 Impact of Rack-to-Fuel assembly

For structure to which the ASME Section III, Subsection NF [Ref. A.2] is applied, there is no requirement for secondary stress. But evaluation for impact was performed to guarantee that local collision does not affect critical state of stored fuel. Integrity of local rack wall was evaluated conservatively using peak impact load. Limit impact load to induce overall permanent deformation was calculated by plastic analysis.

The new and spent fuel storage rack wall allows side load of maximum 273.2kN (61,410 lbf) and 47.4kN (10,660 lbf), respectively. Maximum impact load of fuel assembly is 3.5kN (798 lbf) and 10.1kN (2,273 lbf) as shown in Table 8.4, therefore rack wall is satisfied with allowable load.

8.2 Stress Evaluation

In this section, structural integrity for weld and each part of rack was evaluated by using the maximum load in vertical and horizontal direction determined by time history analysis result of fuel storage rack. Evaluation results according to stress allowable criteria are summarized as follows.

8.2.1 Stress Evaluation of Rack

Stress of rack cell and support pedestal for maximum load in horizontal and vertical direction of support pedestal was evaluated for stress combination which is the greatest load combination in ASME Section III, Subsection NF. Stress coefficient calculations of new and spent fuel storage rack are evaluated based on maximum applied load. Rack and support pedestal stress is lower than allowable criteria 1. Therefore, it is satisfied with the allowable criteria.

Table 8.5 Maximum Stress Coefficient of New Fuel Storage Rack

	Service Condition	Support Pedestal	Rack Cell	Remark
New Fuel Storage Rack	Level A	0.555	0.242	
	Level D	0.344	0.139	

Table 8.6 Maximum Stress Coefficient of Spent Fuel Storage Rack

	Service Condition	Support Pedestal	Rack Cell	Remark
Region I	Level A	0.251	0.326	
	Level D	0.246	0.388	
Region II	Level A	0.238	0.61	
	Level D	0.178	0.645	

8.2.2 Stress Evaluation of Weld

8.2.3.1 Rack cell-to-bottom plate weld

Rack cell-to-bottom plate weld is evaluated multiplying calculated maximum stress coefficient by converted coefficient of actual cross section of rack to weld cross section ratio, then was compared with weld allowable stress value of each load condition.

$$\text{Stress Intensity Coefficient (Ratio)} = \frac{(220+2.5)\times 2.5}{180\times 2.5\times 0.707} = 1.748$$

Where, Inner cell dimension [220 mm (8.66 in.)], Cell thickness [2.5 mm (0.098 in.)],
Weld length [190 mm (7.48 in.)], Weld thickness [2.5 x 0.707 = 1.767 mm (0.069 in.)]

For conservative evaluation, combination of load generating the greatest stress in weld of cell-to-bottom plate was calculated by sum of square stress for shear and stress coefficient of member, which receive bending and axial compression at the same time. Stress coefficient of cell wall calculated based on each load case can be converted to acting stress on the weld of cell-to-cell as follows:

For Level A Condition

$$\sqrt{(FACT2\times 0.6)^2+(FACT3\times 0.6)^2}\times Sy\times Ratio$$

$$= \sqrt{(0.61\times 0.6)^2+(0.11\times 0.6)^2}\times 21400\times 1.748 = 13913 \text{ psi}$$

For Level D Condition

$$\sqrt{(FACT2\times 1.2)^2+(FACT3\times 1.2)^2}\times Sy\times Ratio$$

$$= \sqrt{(0.645\times 1.2)^2+(0.131\times 1.2)^2}\times 21400\times 1.748 = 29545 \text{ psi}$$

Therefore, calculated stress on the weld of cell-to-bottom plate of rack is summarized is as below. It is satisfied with design criteria of weld because safety coefficient is greater than 1.

Service Condition	Calculated Stress (psi)	Allowable Stress (psi)	Safety Factor
Level A	13913	19830	1.42
Level D	29545	35694	1.21

8.2.3.2 Base plate-to-support pedestal weld

For conservative evaluation, stress of base plate-to-support pedestal weld was evaluated using maximum support pedestal load of new fuel storage rack and dimension of support pedestal welds of spent fuel storage rack. Weld stress was calculated by combining the horizontal load based on dynamic analysis with maximum tensile load which is obtained from ANSYS (Ref. E.1). Detailed calculation results are summarized as follows:

Service Condition	Calculated Stress (psi)	Allowable Stress (psi)	Safety Factor
Level A	12369	19830	1.60
Level D	17992	35748	1.98

8.2.3.3 Rack cell-to-cell weld

Stress of rack cell-to-cell weld is calculated by combination of shear stress due to horizontal load acting on rack and shear stress due to impact load of rack cell-to-fuel assembly. Stress of rack cell-to-cell weld was conservatively evaluated by comparing Level A allowable value with SSE load condition, calculation results are as follows.

Portion	Calculated Stress (psi)	Allowable Stress (psi)	Safety Factor
Weld	6567	19830	3.02
Cell	4652	8560	1.84

9.0 Conclusions

Seismic and structural analysis results of high density fuel storage rack of the APR1400 are as follows.

1. Because maximum relative displacement 42. 8 mm (1.684 in.) of Region I and 4.8 mm (0.187 in.) of Region II racks is within installation gaps between rack cells, collision does not occur.

2. Stress coefficient of support pedestal and rack is within allowable stress limit.

3. Calculated stress in rack weld exists within allowable stress value.

Therefore, New and spent fuel storage rack of the APR1400 satisfy the structural integrity requirements under Level A, Level B and Level D conditions.

10.0 References

A. Codes / Standards

1. USNRC NUREG-0800, Standard Review Plan, May 2010.
2. ASME Boiler and Pressure Vessel Code, Section III Rules for Construction of Nuclear Power Plant Component, 2007 Edition with 2008 Addenda
3. ASME Boiler and Pressure Vessel Code, Section II, Material Specification, 2007 Edition with 2008 Addenda
4. Regulatory Guide 1.13, Spent Fuel Storage Facility Design Basis, Rev.2, U.S. Nuclear Regulatory Commission, March 2007.
5. Regulatory Guide 1.92, “Combining Modal Responses and Spatial Components in Seismic Response Analysis”, Rev. 2, U.S. Nuclear Regulatory Commission, July 2006.

B. Specifications / Contract Documents

1. Korea Power Engineering Company, Inc. KOPEC Job No. 2L179, Project Technical Specification 9-423-N224, "New and Spent Fuel Storage Racks", Revision 2 with Addendum 1 dated December 29, 2009.
2. KEPCO E&C Memo No.MES/HS-130001M, “SFP & NFSA ISRS”, March 18, 2013.

C. Textbooks

1. Timoshenko, S.P., "Strength of Materials”, 3rd Edition, Part II.

D. Papers

1. S. Singh, et. Al., "Structural Evaluation of Onsite Spent Fuel Storage: Recent Developments", Proceedings of the Third Symposium, Orlando, Florida, December 1990, North Carolina State University, Raleigh, NC 27695, pp V/4-1 through V/4-18.
2. Fritz, R.J., "The Effects of Liquids on the Dynamic Motions of Immersed Solids", Journal of Engineering for Industry, Trans. of ASME, February 1972, pp 167-172.
3. Rabinowicz, E., "Friction Coefficients of Water Lubricated Stainless Steels for a Spent Fuel Rack Facility", MIT, a Report for Boston Edison Company, 1976.

E. Computer Programs / Manuals

1. Computer code, ANSYS Version 10.0; Installed on HP Integrity Superdome 16 Way of Hewlett Packard Co., Verification Document No. DAVM100, Rev.0, July 2006.
2. Computer code, ATIGEN Version 0; Installed on PC of Hewlett Packard Co., Verification Document No. NBOP-FR-CV-001, Rev.0, August 8, 2008.
3. Computer code, STCOR Version 0; Installed on PC of Hewlett Packard Co., Verification Document No. NBOP-FR-CV-002, Rev.0, August 8, 2008.

F. Drawings

1. N13027-224CD-1000, Rev.0, New Fuel Storage Pit Layout
2. N13027-224CD-2000, Rev.0, Spent Fuel Pool Layout